CHAPTER 4

IMPEDANCE SPECTROSCOPY MEASUREMENTS AND CONDUCTIVITY

Introduction

A very important study concerning conductors is electrical conductivity. Many researchers have been studying electrical conductivity in order to understand the transport mechanism. By understanding how the charges are transported, possible applications of such materials can be considered.

Since in this work, the pelletized xCuI-(1-x)AgI, ($0.1 \leq x \leq 0.4$) samples were prepared by sintering at the temperature of 250°C. Pellets with a fixed weight percent were prepared. The composition that gives the highest room temperature conductivity for xCuI-(1-x)AgI, ($0.1 \leq x \leq 0.4$) binary system will be determined. As mentioned in Chapter Three, the electrical conductivity can be calculated using the bulk resistance, R_b which can be determined from the complex impedance plot. The pellets that will be tested were kept in silica gel containing desiccators to ensure the dryness of the pellets. Each pellet were sandwiched between two stainless steel electrodes and placed in the conductivity mount with leads to the bridge. The entire set up was kept inside a desicator.

4.1 Conductivity Studies

4.1.1 Composition Dependence of conductivity in the *x*CuI-(1-x)AgI system

The room temperature electrical conductivity was measured using impedance spectroscopy. Figures 4.1 to 4.5 display the complex impedance plots for all samples at room temperature. The imaginary impedance, Z_i versus real impedance, Z_r plot on the low frequency side of the semicircle gives the bulk resistance, R_b of the system. Three replicates of each composition were used in impedance measurement.

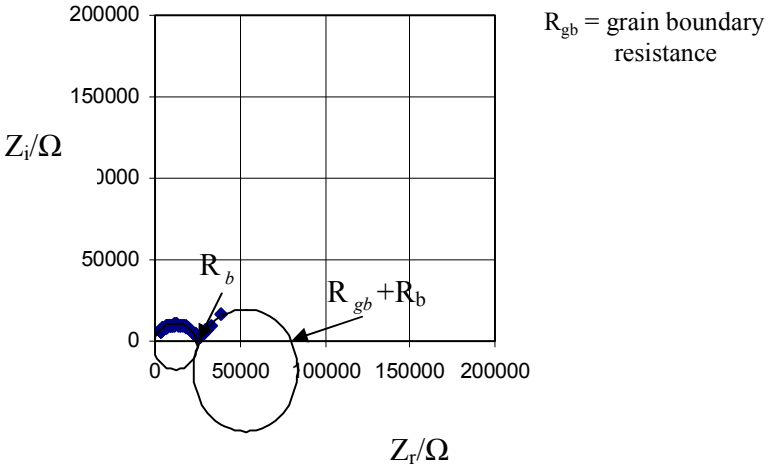

Figure 4.1: complex impedance plot of pure AgI at room temperature.

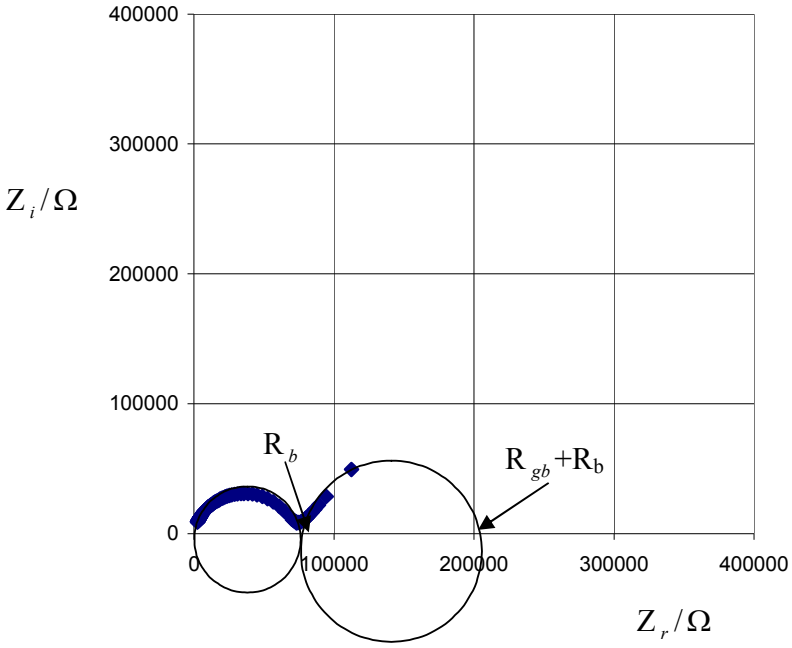

Figure 4.2: complex impedance plot of 0.1CuI-0.9AgI at room temperature.

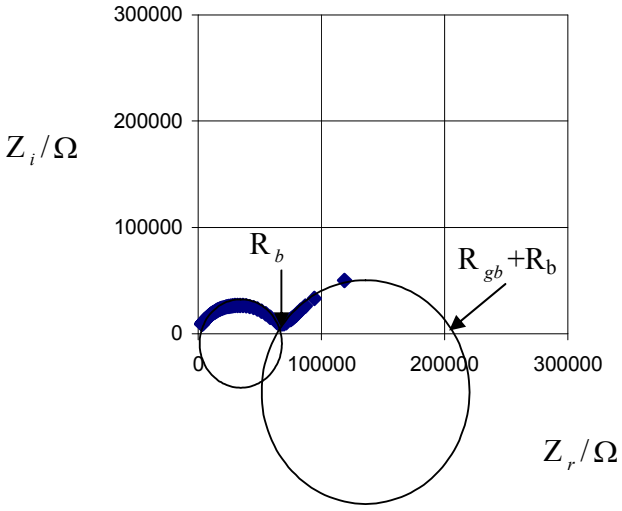

Figure 4.3: complex impedance plot of 0.2CuI-0.8AgI at room temperature.

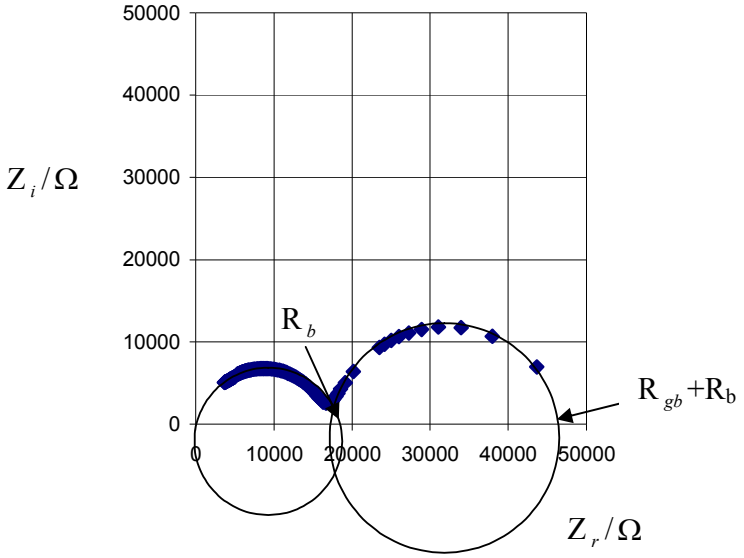

Figure 4.4: complex impedance plot of 0.3CuI-0.7AgI at room temperature.

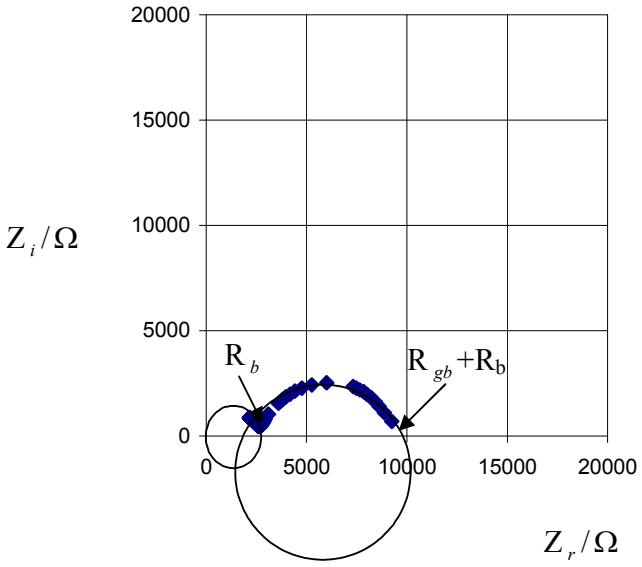

Figure 4.5: complex impedance plot of 0.4CuI-0.6AgI at room temperature.

From the complex impedance spectrum of the samples, the values of bulk resistance, R_b and grain boundary resistance, R_{gb} can be determined. Table 4.1 lists the values of R_b and R_{gb} of the pellets.

Table 4.1: R_b and R_{gb} of xCuI-(1-x)AgI, ($0 \leq x \leq 0.4$) system.

Sample	R_b (Ω)	R_{gb} (Ω)
$x = 0$	$(2.51 \pm 0.74) \times 10^4$	$(5.87 \pm 0.19) \times 10^4$
$x = 0.1$	$(1.66 \pm 0.50) \times 10^5$	$(1.58 \pm 0.49) \times 10^6$
$x = 0.2$	$(1.26 \pm 0.07) \times 10^5$	$(7.17 \pm 0.18) \times 10^5$
$x = 0.3$	$(1.28 \pm 0.36) \times 10^4$	$(2.75 \pm 0.80) \times 10^4$
$x = 0.4$	$(2.84 \pm 0.64) \times 10^3$	$(1.31 \pm 0.03) \times 10^4$

From Table 4.1, using the value of R_b the electrical conductivity can be calculated from the equation:

$$\sigma = \frac{t}{R_b A}$$

It can be seen that the sample containing 0.4CuI-0.6AgI exhibited the smallest bulk resistance, R_b. Hence, the sample will exhibit the highest conductivity at room temperature.

The centre of the semicircle is noted to be below the Z_r axis indicating that the material can be represented by an equivalent circuit comprising of a resistor and a capacitor whose capacitance changes with frequency (Linford, 1988). From the plots, two depressed or tilted semicircles can be expected. In Figures 4.1 to 4.5, two semicircles can be expected. The first semicircle is observed in all samples. The high frequency is on the left hand side of the semicircle and the lower frequency is to the right hand side of the semicircle. On the low frequency side of the first semicircle where the plot tends to cut the Z_r-axis is the value

of the bulk resistance, R_b. On the low frequency side of the second semicircle, the plot gives the bulk resistance, R_b and grain boundary resistance, R_{gb}. The appearance of the semicircle is more obvious on addition of more CuI.

Table 4.2 lists the conductivity value for all compositions studied at room temperature. The highest conductivity is 1.75×10^{-5} S cm^{-1}.

Table 4.2: Conductivities of AgI-CuI mixture at room temperature.

Sample	Content of AgI salt (wt%)	Content of CuI salt (wt%)	Conductivity, S/cm
A1	100	0	$(2.00 \pm 0.50) \times 10^{-6}$
A2	90	10	$(4.68 \pm 0.18) \times 10^{-7}$
A3	80	20	$(7.24 \pm 0.23) \times 10^{-7}$
A4	70	30	$(4.59 \pm 1.61) \times 10^{-6}$
A5	60	40	$(1.75 \pm 0.10) \times 10^{-5}$

Conductivity variation with CuI content is as shown in Figure 4.6.

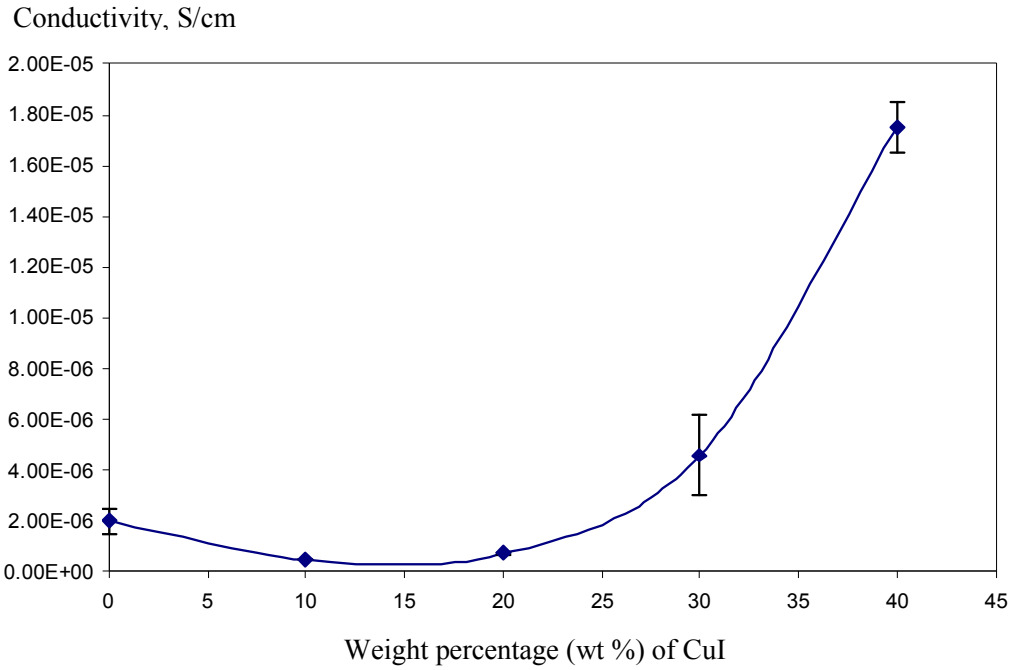

Figure 4.6: Plot of conductivity at room temperature

It can be observed from Figure 4.6 that the conductivity decreases from pure AgI to 0.1CuI-0.9AgI. Electrical conductivity of *x*CuI-(1-*x*)AgI binary system started to increase with addition of more than 20 wt. % CuI into the binary system. Highest room temperature conductivity is found to be $1.75 \times 10^{-5}\,\mathrm{Scm}^{-1}$.

4.1.2 Frequency dependence of electrical conductivity, σ (ω)

It is well known that the conductivity of superionic conductors depends on temperature. Conductivity of *x*CuI-(1-*x*)AgI binary system have been measured at temperatures from 25°C to 150°C. It can be seen that the conductivity increases with

increasing temperature. The frequency dependence of electrical conductivity, σ(ω) in *x*CuI-(1-*x*)AgI can usually be well described using Jonscher's expression (Correa et.al., 2007):

$$\sigma(\omega) = \sigma_{dc}\left[1 + \left(\frac{j\omega}{\omega_p}\right)^n\right] \tag{4.1}$$

where σ_{dc} is the dc conductivity, ω_p is a characteristic relaxation or crossover frequency, n is a fractional exponent between 0 and 1. Thus, a non-dispersive dc conductivity σ_{dc} is expected for $\omega \leq \omega_p$ and a crossover to a power law dependent ac conductivity of the form ω^n when frequency is greater than ω_p.

σ(ω) versus frequency for pure AgI at temperatures investigated are shown in Figure 4.7(*a*) to 4.7(*l*).

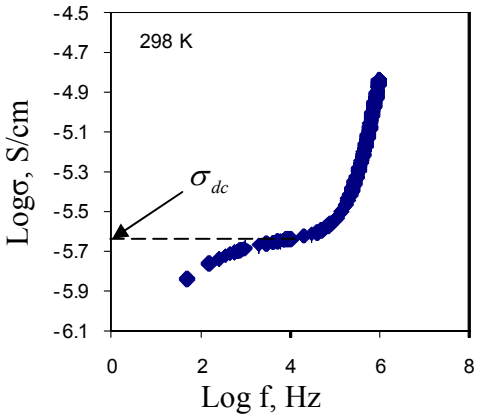

Figure 4.7(*a*)

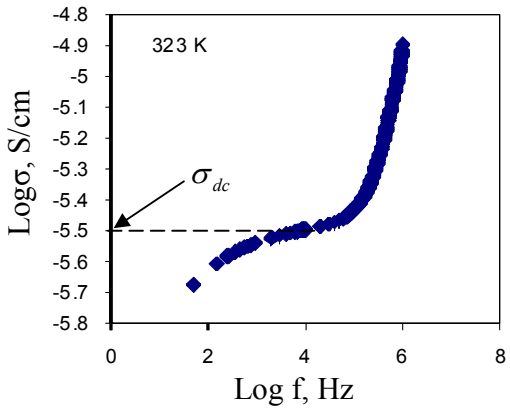

Figure 4.7(*b*)

Continue…

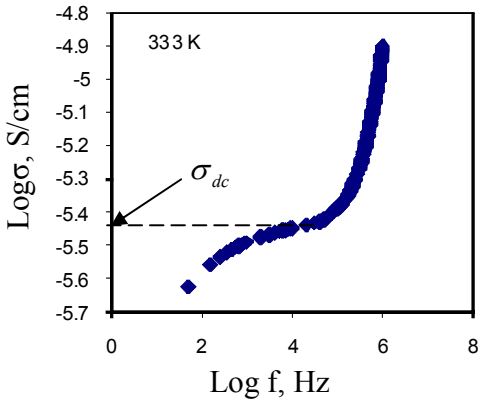

Figure 4.7(*c*)

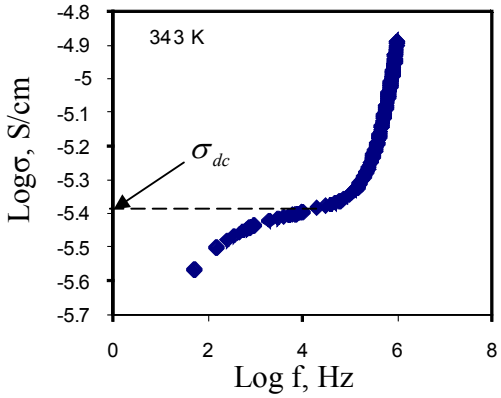

Figure 4.7(*d*)

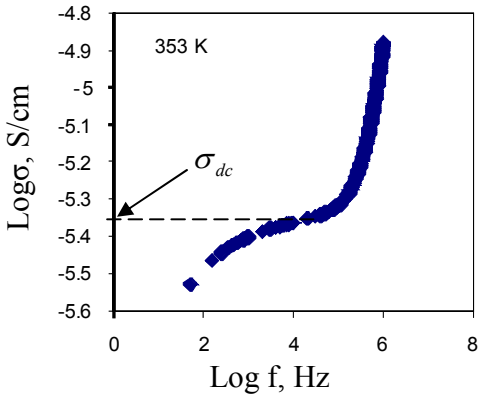

Figure 4.7(*e*)

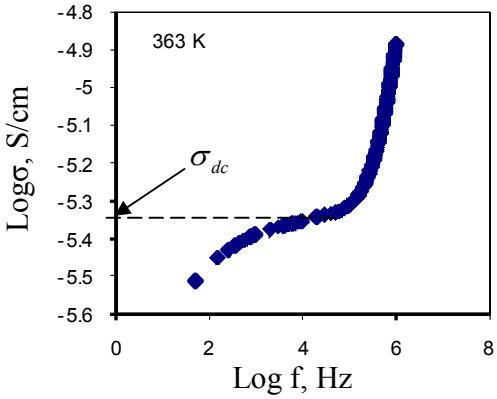

Figure 4.7(*f*)

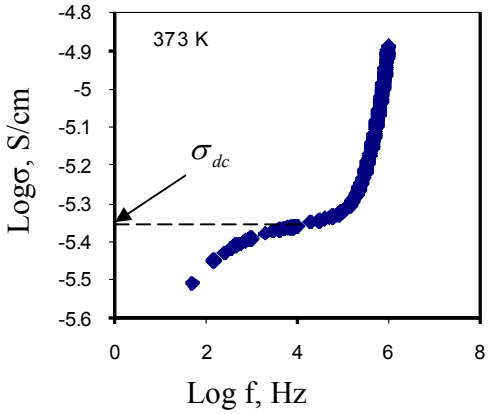

Figure 4.7(*g*)

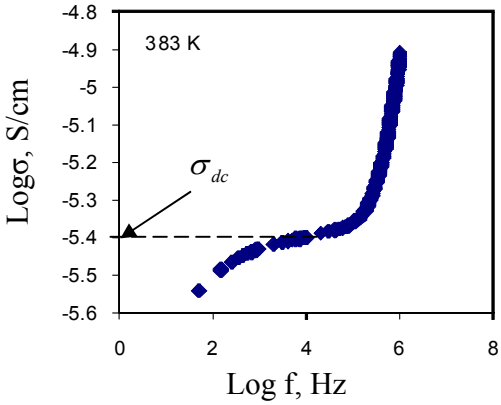

Figure 4.7(*h*)

Continue...

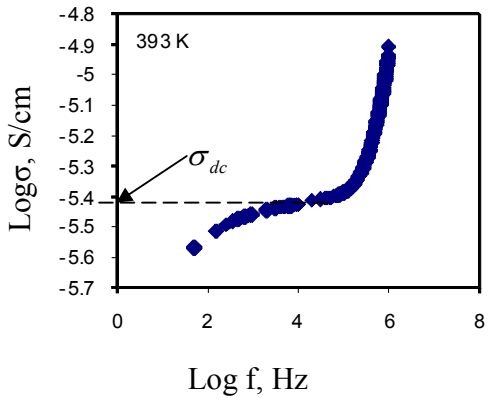

Figure 4.7(*i*)

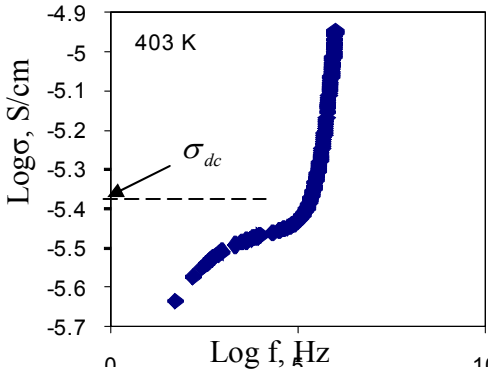

Figure 4.7(*j*)

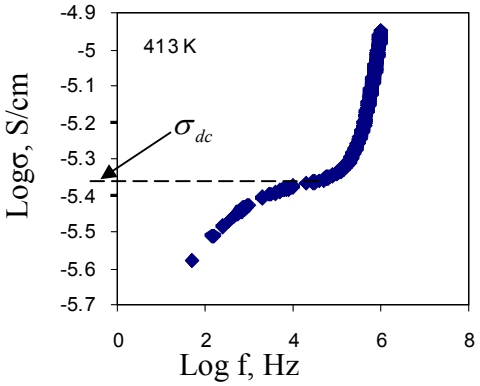

Figure 4.7(*k*)

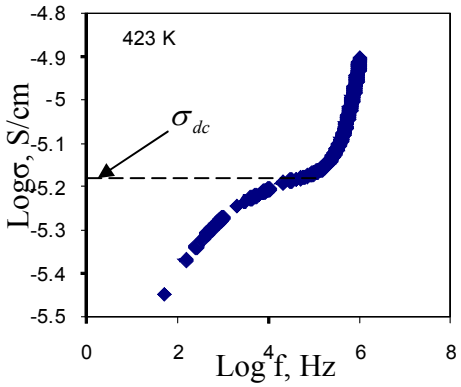

Figure 4.7(*l*)

Figure 4.7: Plots of frequency dependent of conductivity $\sigma(\omega)$ at several temperatures for pure AgI.

Overall three distinct regions can be observed in the log σ versus log f graphs where between 1< log f < 4 the conductivity decreases with frequency, between 4< log f < 5, conductivity is quite independent of frequency and for log f > 5 where conductivity increases with frequency.

σ(ω) versus frequency for 0.1CuI-0.9AgI at temperatures investigated are shown in Figure 4.8(*a*) to 4.8(*l*).

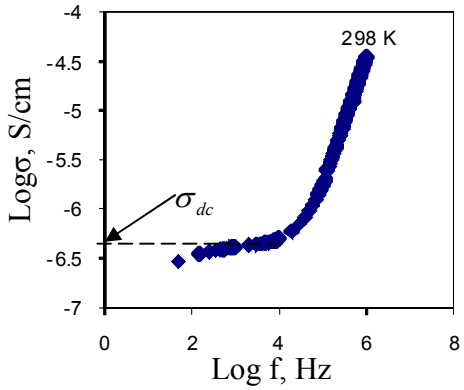

Figure 4.8(*a*)

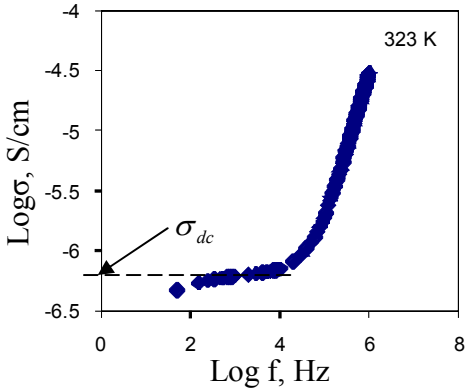

Figure 4.8(*b*)

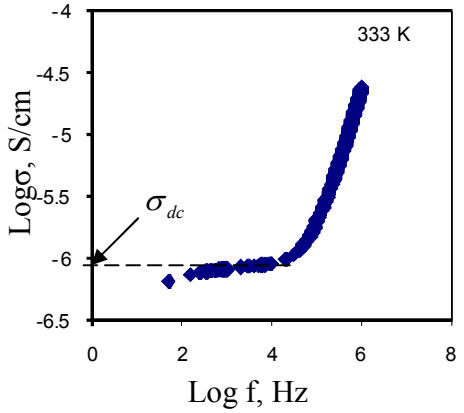

Figure 4.8(*c*)

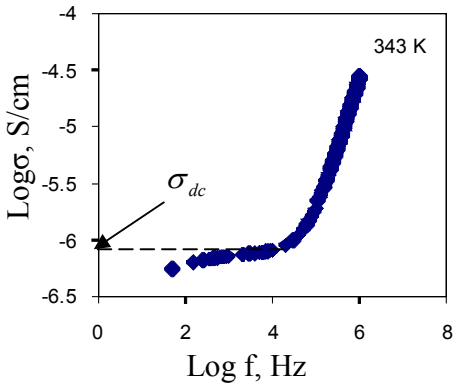

Figure 4.8(*d*)

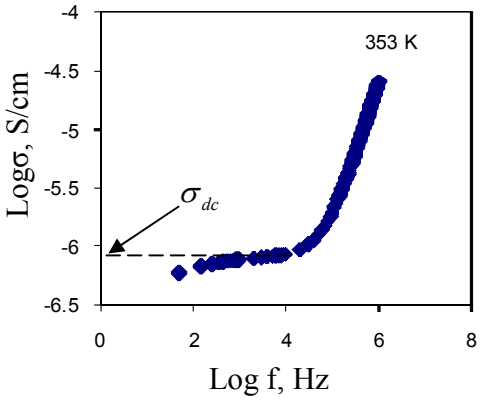

Figure 4.8(*e*)

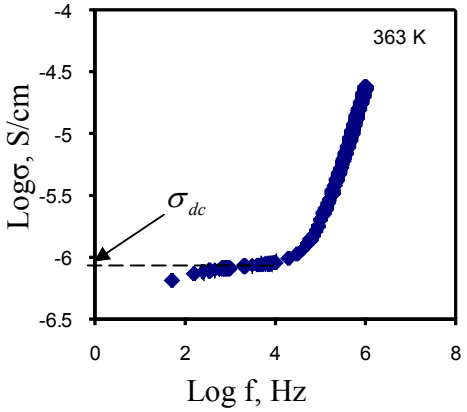

Figure 4.8(*f*)

Continue…

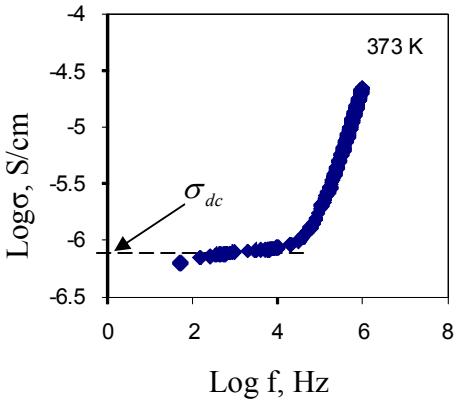

Figure 4.8(*g*)

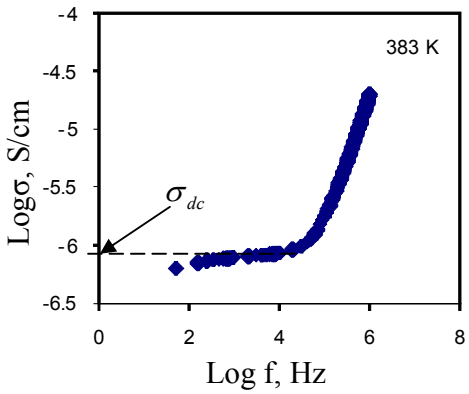

Figure 4.8(*h*)

403 K

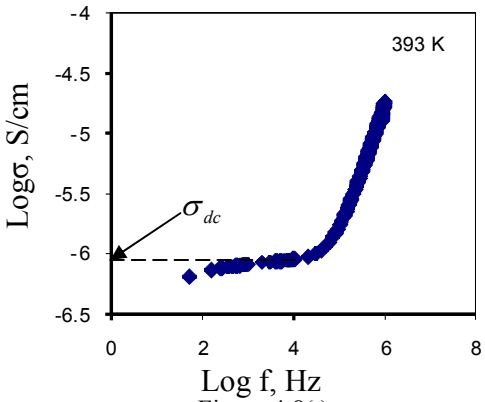

Figure 4.8(*i*)

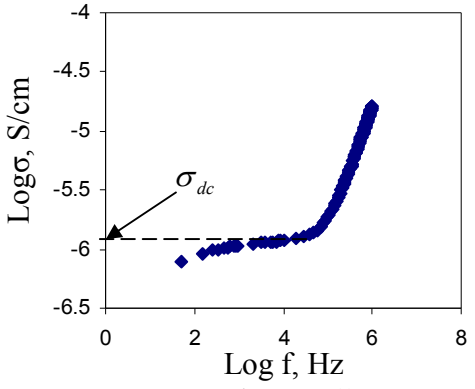

Figure 4.8(*j*)

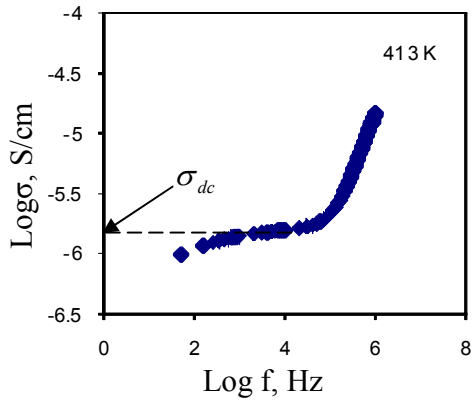

Figure 4.8(*k*)

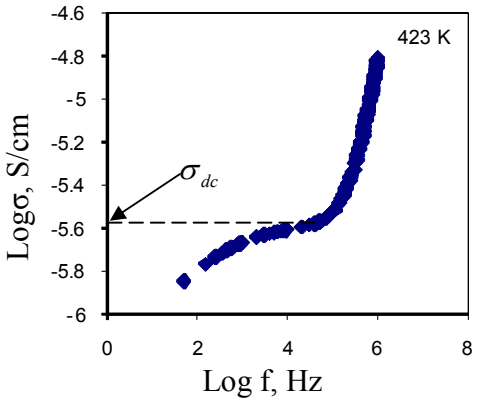

Figure 4.8(*l*)

Figure 4.8: Plots of frequency dependent of conductivity $\sigma(\omega)$ at several temperatures for 0.1CuI-0.9AgI.

Again three distinct regions can be distinguished.

σ(ω) versus frequency for 0.2CuI-0.8AgI at temperatures investigated are shown in Figure 4.9(*a*) to 4.9(*l*).

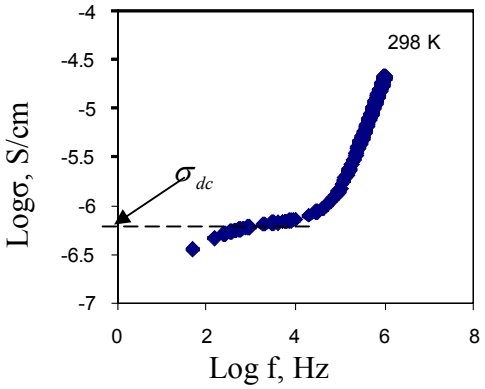

Figure 4.9(*a*)

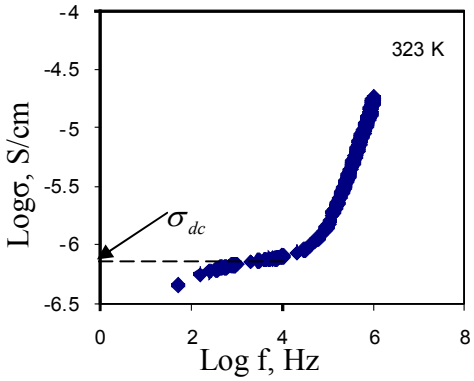

Figure 4.9(*b*)

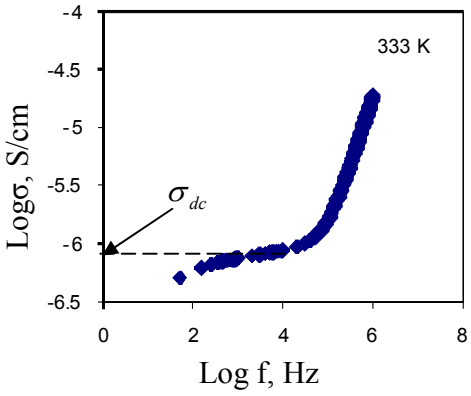

Figure 4.9(*c*)

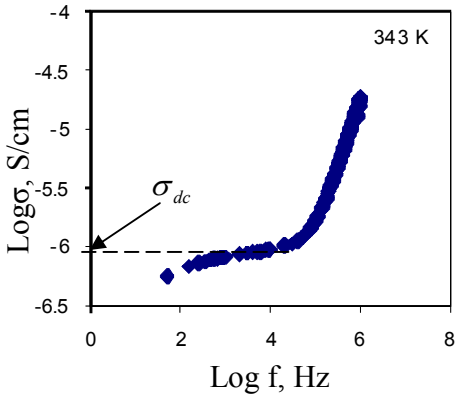

Figure 4.9(*d*)

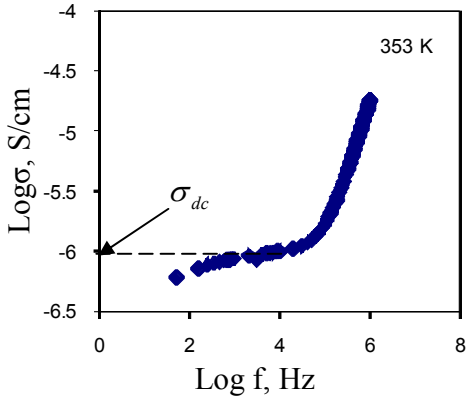

Figure 4.9(*e*)

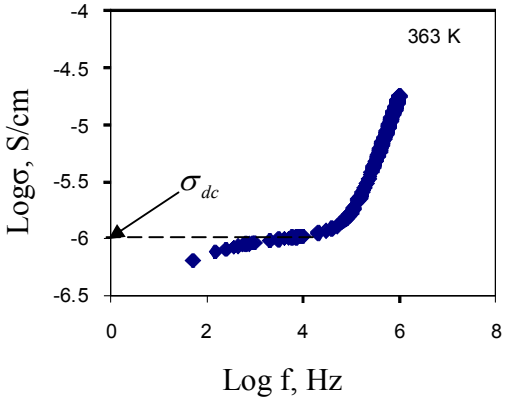

Figure 4.9(*f*)

Continue …

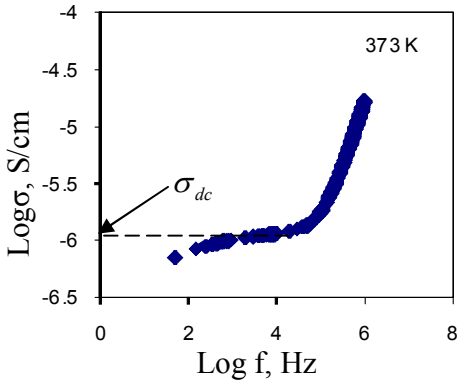

Figure 4.9(*g*)

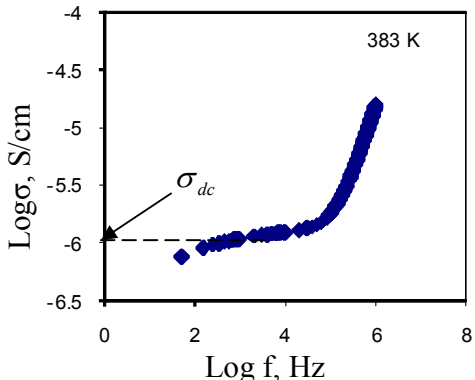

Figure 4.9(*h*)

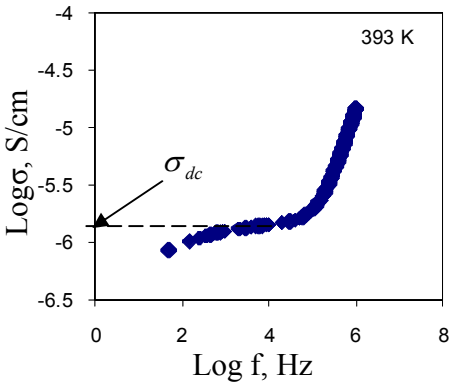

Figure 4.9(*i*)

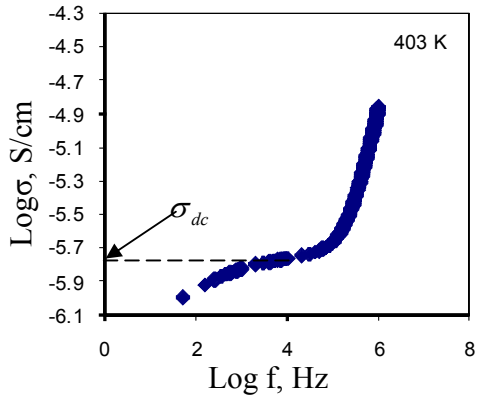

Figure 4.9(*j*)

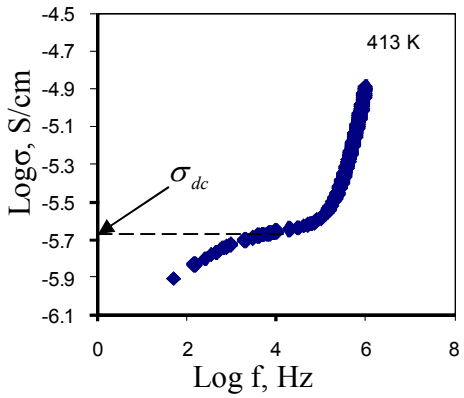

Figure 4.9(*k*)

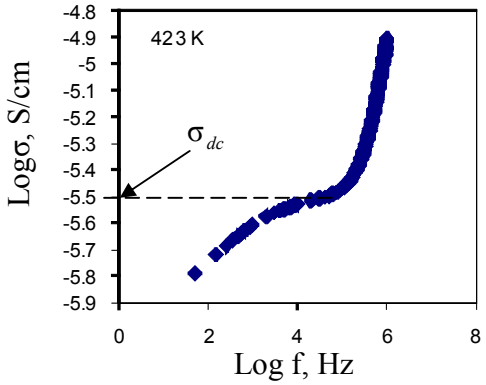

Figure 4.9(*l*)

Figure 4.9: Plots of frequency dependent of conductivity $\sigma(\omega)$ at several temperatures for 0.2CuI-0.8AgI.

Three distinguished regions can still be observed but at high temperatures the region where the conductivity is independent, frequency is quite short especially at 423 K.

σ(ω) versus frequency for 0.3CuI-0.7AgI at temperatures investigated are shown in Figure 4.10(*a*) to 4.10(*l*).

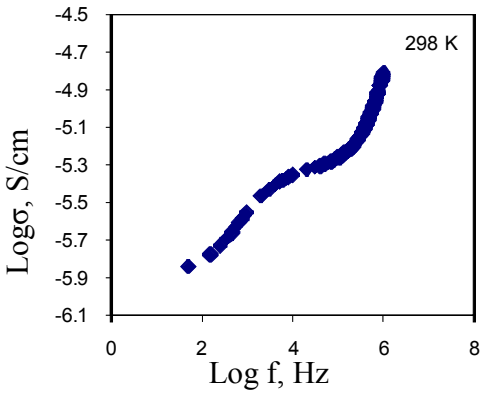

Figure 4.10(*a*)

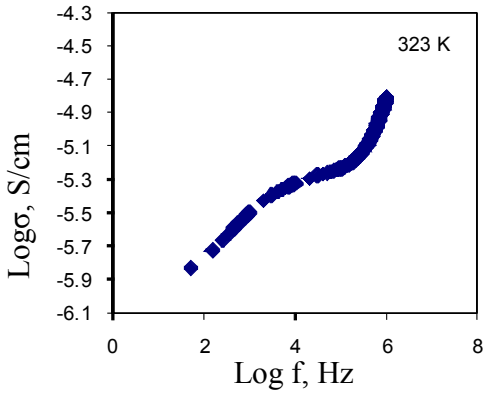

Figure 4.10(*b*)

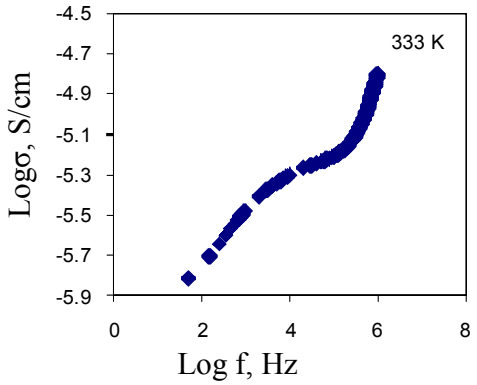

Figure 4.10(*c*)

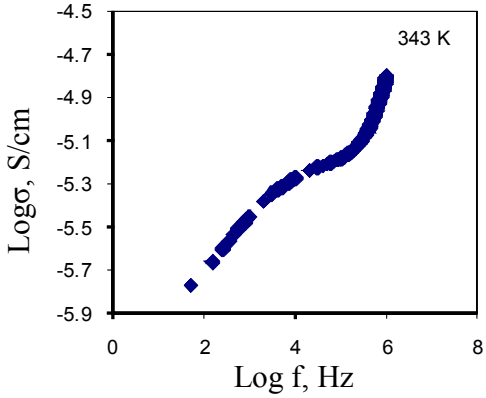

Figure 4.10(*d*)

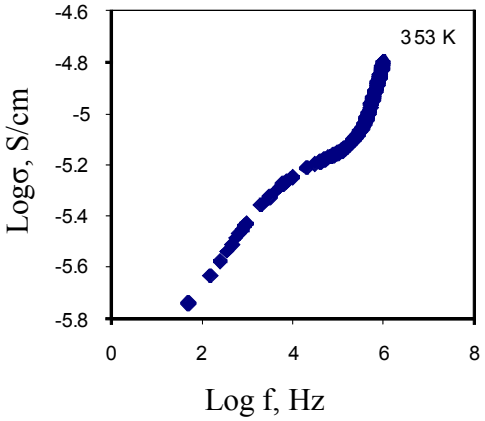

Figure 4.10(*e*)

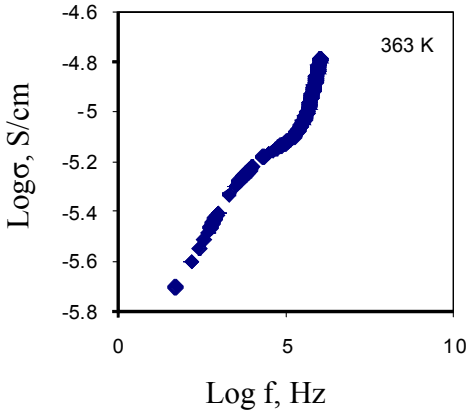

Figure 4.10(*f*)

Continue …

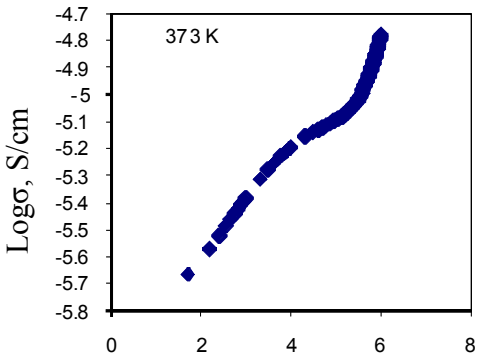

Figure 4.10(*g*)

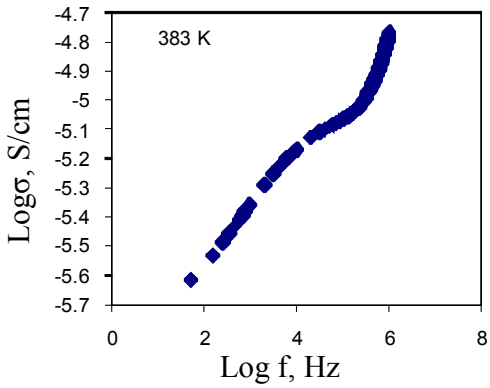

Figure 4.10(*h*)

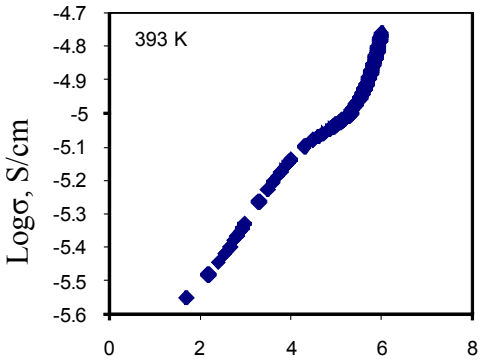

Figure 4.10(*i*)

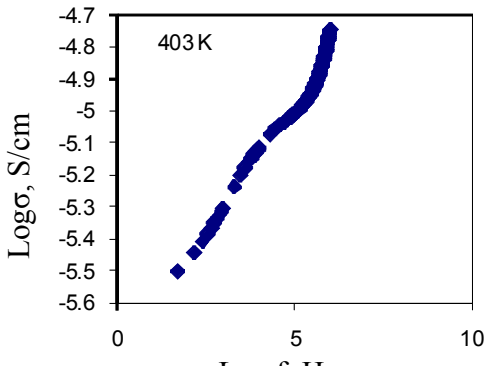

Figure 4.10(*j*)

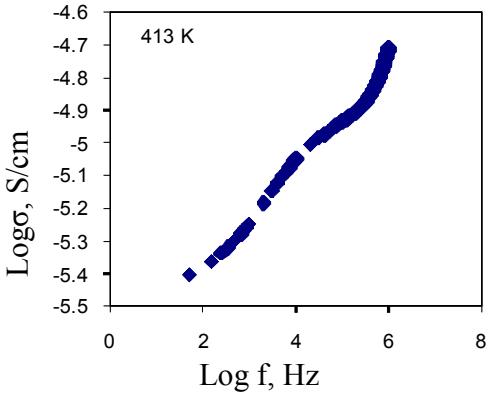

Figure 4.10(*k*)

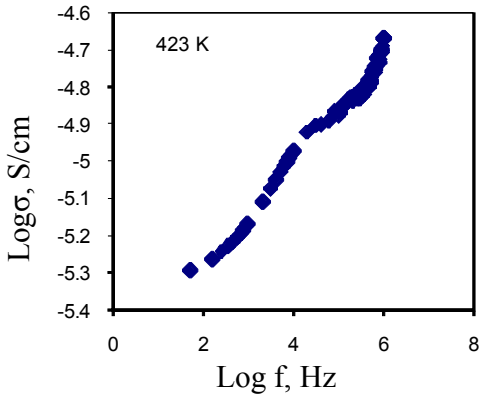

Figure 4.10(*l*)

Figure 4.10: Plots of frequency dependent of conductivity $\sigma(\omega)$ at several temperatures for 0.3CuI-0.7AgI.

As the amount of CuI increases to 30 wt%, the conductivity independent of frequency region is not quite noticeable.

σ(ω) versus frequency for 0.4CuI-0.6AgI at temperatures investigated are shown in Figure 4.11(*a*) to 4.11(*l*).

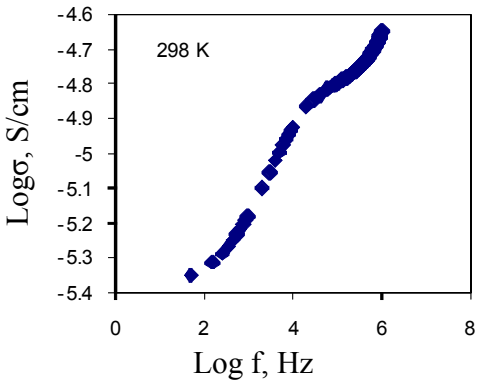

Figure 4.11(*a*)

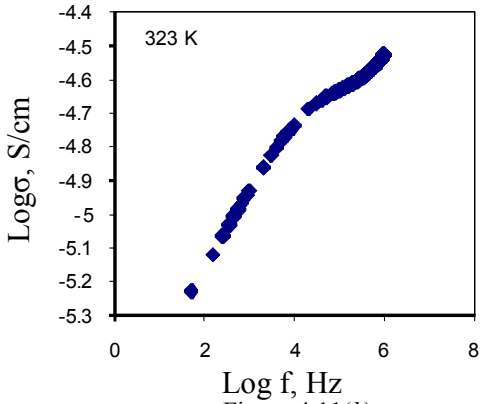

Figure 4.11(*b*)

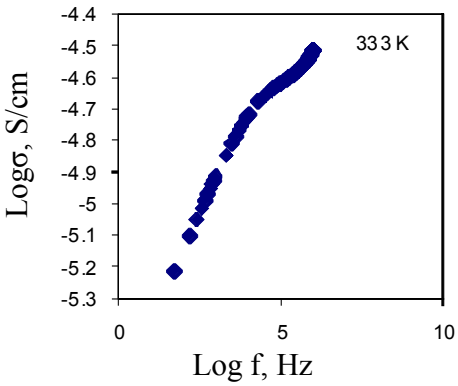

Figure 4.11(*c*)

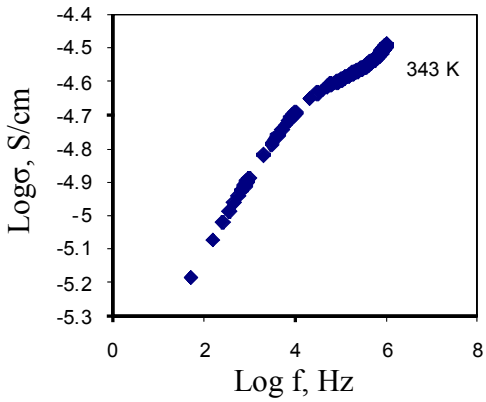

Figure 4.11(*d*)

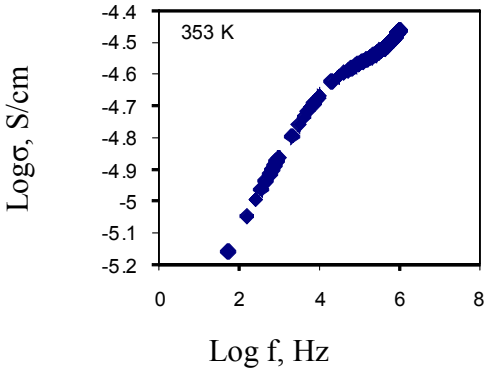

Figure 4.11(*e*)

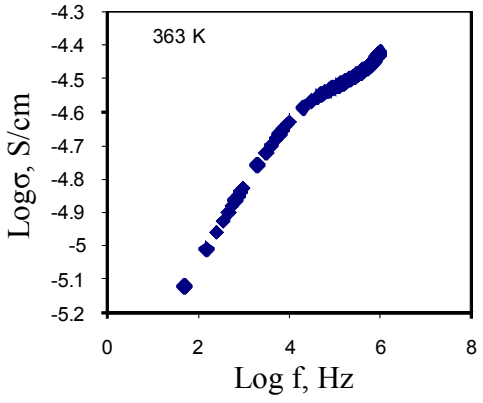

Figure 4.11(*f*)

Continue …

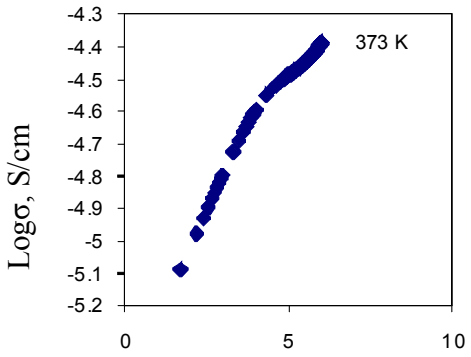

Figure 4.11(*g*)

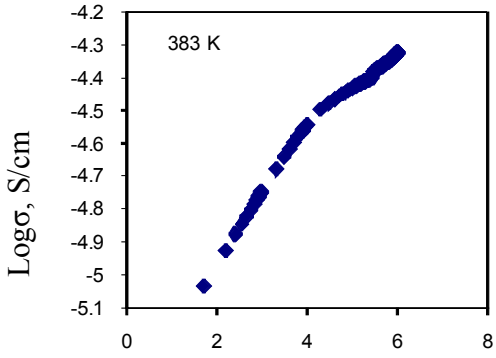

Figure 4.11(*h*)

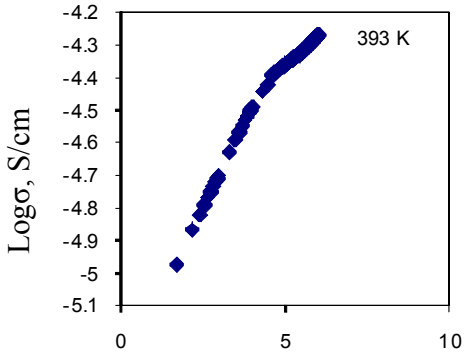

Figure 4.11(*i*)

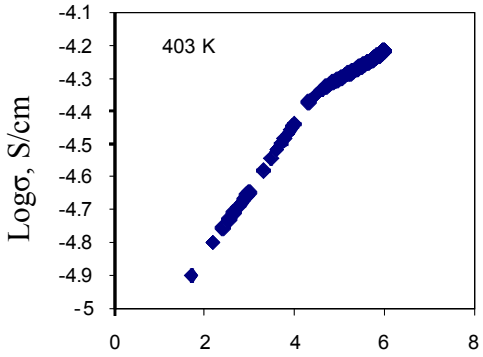

Figure 4.11(*j*)

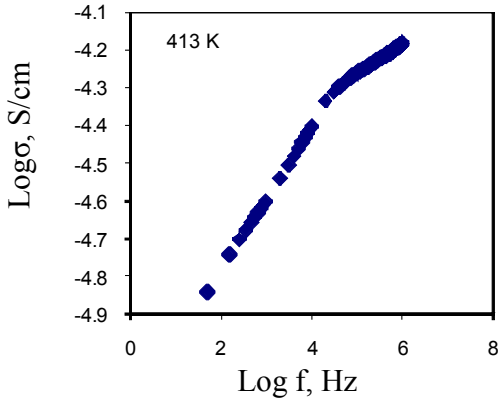

Figure 4.11(*k*)

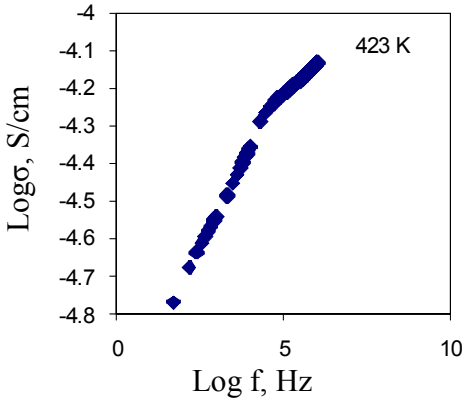

Figure 4.11(*l*)

Figure 4.11: Plots of frequency dependent of conductivity $\sigma(\omega)$ at several temperatures for 0.4CuI-0.6AgI.

Once again the conductivity-frequency independent region is not easily observed.

4.1.3 σ_{dc} and temperature relationship

The conductivity for the samples was measured at different temperatures from 298 K to 423 K. This temperature range covers the transmission temperature for γ- to β-AgI.

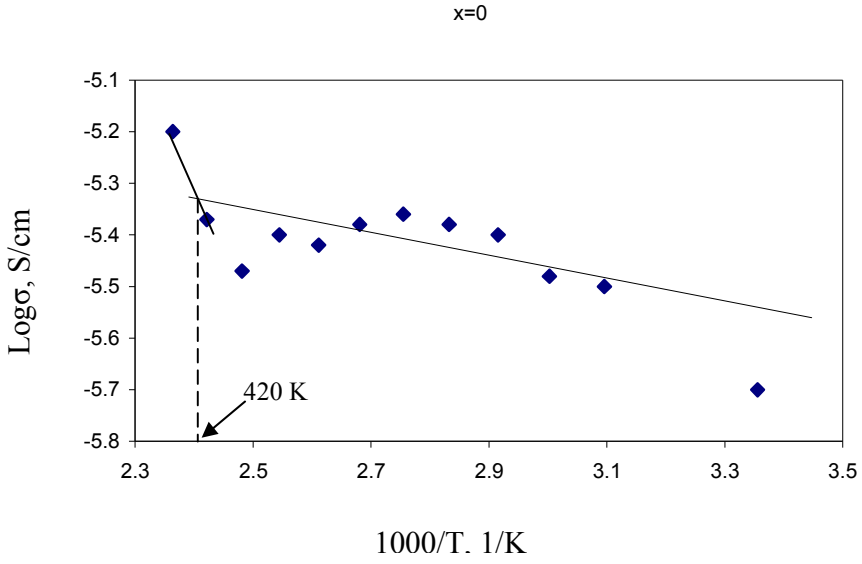

Figure 4.12: Temperature dependence of ionic conductivity for pure AgI.

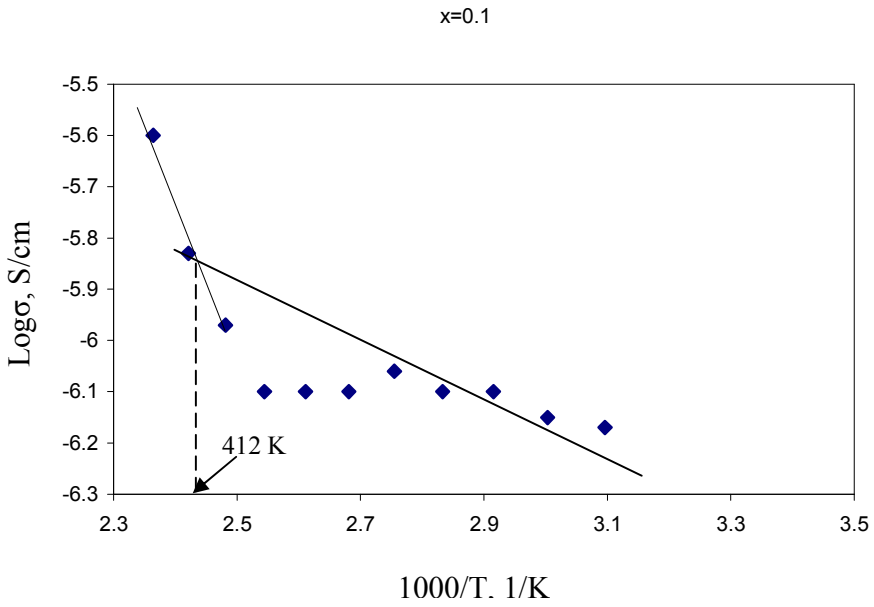

Figure 4.13: Temperature dependence of ionic conductivity for 0.1CuI-0.9AgI.

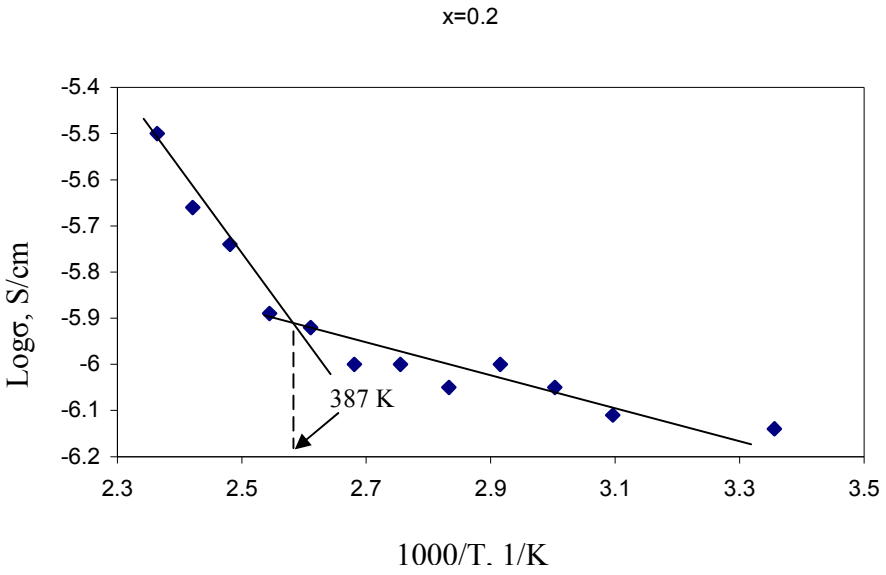

Figure 4.14: Temperature dependence of ionic conductivity for 0.2CuI-0.8AgI.

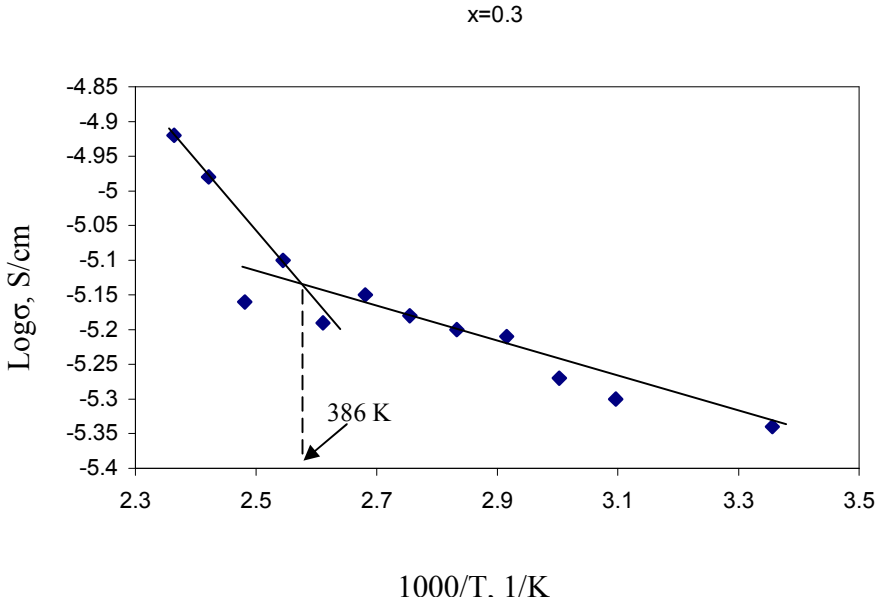

Figure 4.15: Temperature dependence of ionic conductivity for 0.3CuI-0.7AgI.

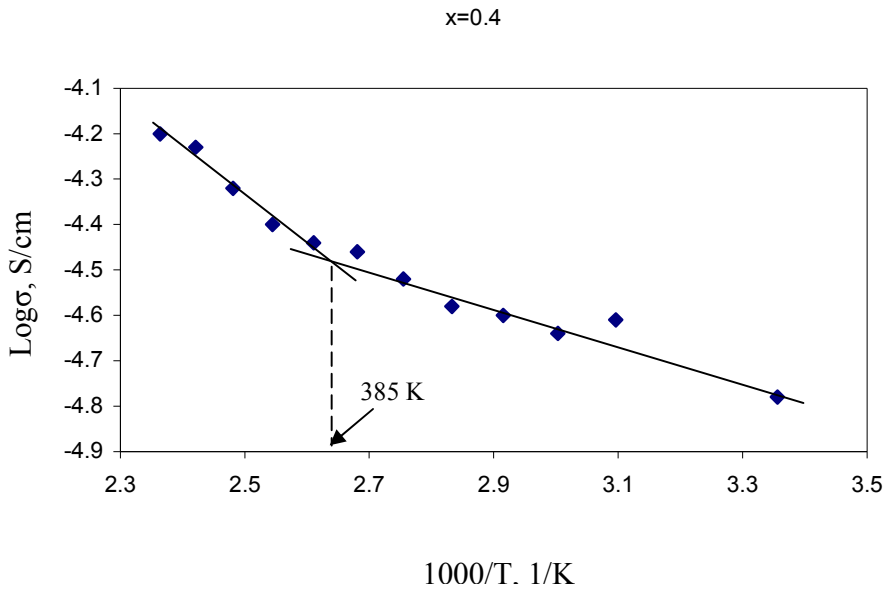

Figure 4.16: Temperature dependence of ionic conductivity for 0.4CuI-0.6AgI.

AgI-CuI samples with 0 wt% to 40 wt% CuI in the binary system have been measured. In order to understand the conductivity mechanism in Ag-CuI system, the conductivity was measured at different temperatures. In the pure AgI system, a sharp increase in conductivity at temperature of 420 K is observed. The sharp increase in conductivity is attributed to the phase transition of γ-AgI or β-AgI to superionic α-AgI. For the system which contains 0.1CuI-0.9AgI, the conductivity shows a sharp increment at 412 K, for 0.2CuI-0.8AgI at 387 K, for 0.3CuI-0.7AgI at 386 K and for the 0.4CuI-0.6AgI at 385 K. It can be seen that the addition of CuI into the binary system lowers the phase transition temperature of β to α-AgI. This means that with more CuI added to the system, the phase transition of β to α-AgI occurs at a lower temperature. However the d.c conductivity for 250 °C sintered pure AgI, 0.1CuI-0.9AgI and 0.2CuI-0.8AgI at the temperature of investigation are almost similar to the estimated d.c conductivity for the log σ versus log f curve.

4.2 Summary

The AgI-CuI sample that gives the highest room temperature conductivity is 0.4CuI-0.6AgI. The room temperature conductivity is $1.75 \times 10^{-5}\,\mathrm{Scm}^{-1}$. From the graphs log σ versus 1000/T, it can be clearly seen that the conductivity shows a sharp increase at certain temperature. It is believed that the sharp increase is due to the phase transition of β-AgI to α-AgI. With the addition of CuI into the binary system, the temperature of phase transition decreased. Conductivity-temperature relationship is not Arrhenian. Further discussions will be explained in Chapter 7.